



Exergy output rate optimization for an endoreversible Brayton cycle CCHPP

Huijun Feng^{1,2,3}, Lingen Chen^{1,2,3}, Zhihui Xie^{1,2,3}, Yanlin Ge^{1,2,3}

¹ Institute of Thermal Science and Power Engineering, Naval University of Engineering, Wuhan, 430033, P. R. China.

² Military Key Laboratory for Naval Ship Power Engineering, Naval University of Engineering, Wuhan, 430033, P. R. China.

³ College of Power Engineering, Naval University of Engineering, Wuhan 430033, P. R. China.

Received 6 March 2017; Received in revised form 1 June 2017; Accepted 12 June 2017; Available online 1 Sep. 2017

Abstract

A combined cooling, heating and power plant (CCHPP), composed of an endoreversible closed Brayton cycle and absorption refrigerator, is studied in this paper. By introducing the finite time thermodynamics, the formula of the exergy output rate (EOR) of the CCHPP is derived. With the help of Powell arithmetic, the compressor pressure ratio of the Brayton cycle and distributions of 7 heat exchanger heat conductances (HEHCs) are optimized, and the maximum EOR of the CCHPP is obtained. It shows that the hot-side HEHC is the largest one among the discussed HEHCs, and several parameters, such as the total HEHC and ratio of heat reservoir temperature to the surrounding temperature, on the optimal performances of the CCHPP are analyzed.

Copyright © 2017 International Energy and Environment Foundation - All rights reserved.

Keywords: Finite time thermodynamics; CCHPP; Exergy performance; generalized thermodynamic optimization.

1. Introduction

Recently, with the increasingly paying attention on energy and environmental problems, the combined cooling heating and power plant (CCHPP) gradually becomes a topic of interest [1, 2]. Various scholars have investigated the CCHPPs based on the method of classical thermodynamics. Lozano et al. [3] investigated the thermo-economic index of the CCHPP with specified user demand, and obtained the minimum variable cost based on linear programming method. They pointed out that the heat prices had evident effects on the production costs, and the best approach was determined by the issue conditions. Zheng et al. [4] investigated the operation strategy of a CCHPP, and compared the strategy of minimum distance with the other three strategies. They indicated that the performance of the CCHPP and building was well matched, which illustrated the advantage of the minimum distance strategy. Wang et al. [5] studied the energy and exergy performances of a biomass CCHPP, and chose different operational flows according to different seasons. They pointed out that the energy and exergy efficiencies of the biomass CCHPP were 50% and 6.23%, respectively, in summer, and the consumption of the biomass was reduced by 4% when waste heat was recovered. Ju et al. [6] considered the performances of the CCHPP from the viewpoint of energy, economic and environment, and implemented multi-objective optimizations based

on these indexes. The results showed that the CCHPP with distributed energy resource led to the reduction of CO₂ emission when the wind and solar energies were used.

Finite time thermodynamics (FTT) [7-28] has many superiorities in the optimizations of thermodynamic cycles and processes. Lots of scholars optimized the performances of Brayton cycle cogeneration plants (BCCPs) based on FTT. Yilmaz [29] analyzed the exergy output rate (EOR) of a BCCP, and showed that a lower heat consumer temperature led to a higher EOR. Hao and Zhang [30, 31] maximized the useful energy rate and EOR of a BCCP, and showed that the maximum EOR led to a higher EOR performance but a lower exergy efficiency (EE) of the BCCP. Ust et al. [32-34] studied the exergetic performance coefficients (EPCs) of the BCCPs with regenerative Brayton, Dual and Dual Miller cycles, respectively, and showed that the results of the BCCPs obtained based on maximum EPC had a superiority in the aspect of entropy generation rate. Tao et al. [35, 36] and Chen et al. [37] investigated the exergoeconomic performances (EPs) of the endoreversible [35, 36] and irreversible [37] BCCPs, and found that their performances could be improved by optimizing heat conductance distributions (HCDs), compressor pressure ratio (CPR) and heat consumer-side temperature, respectively. Yang et al. [38-47] studied the EOR and EP of the endoreversible [38-42] and irreversible [43-47] intercooled regenerative BCCPs, and obtained different optimal HCDs and optimal pressure ratios based on the maximizations of the profit rate and EE of the BCCP, respectively.

Absorption refrigerator is an important part of the CCHPP. Based on FTT analyses of the absorption refrigerators [48-56] and BCCPs [29-47], FTT is also introduced into the performance analyses of the CCHPPs [57, 58]. Chen et al. [57] investigated the EP of a CCHPP with endoreversible closed Brayton cycle (ECBC), and derived the maximum profit rate by choosing the optimal cycle parameters. Yang et al. [58] further implemented exergy analyses of a CCHPP with regenerative ECBC, and pointed out that EOR and EE increased when the regenerator heat conductance (HC) was increased for a small pressure ratio. Based on the model in Ref. [57], the EOR performance of a CCHPP, composed of an ECBC and an endoreversible four-heat-reservoir absorption refrigeration cycle (EFHRARC), will be analyzed in this paper. The EOR will be maximized by varying the HCDs and pressure ratio of the ECBC, respectively, and optimal results will be analyzed at different parameter conditions.

2. Cycle model

Figures 1 and 2 show the model and T-s diagram of the CCHPP, respectively. There are 4 heat reservoirs, and their temperatures are T_H , T_L , T_g' and T_h , respectively. There are 4 processes in the Brayton cycle. Isentropic adiabatic processes locate point 1 to 2 and point 3 to 4, and the working fluid is compressed and expanded in the two processes, respectively. The working fluid receives heat (Q_H) from temperature T_H between point 2 to 3. The working fluid first releases heat (Q_{Kc}) to temperature T_g' of the absorption refrigerator between point 4 and 5, then releases heat (Q_{Kh}) to temperature T_h of the thermal consumer between point 5 to 6, and finally releases heat (Q_L) to temperature T_L of the heat sink. The power output of the CCHPP is P .

The four heat transfer processes above occur in four heat exchangers (HEs). The heat transfer equations of the four HEs can be given as:

$$Q_H = C_{wf}(T_3 - T_2) = C_{wf}E_H(T_H - T_2) \quad (1)$$

$$Q_L = C_{wf}(T_6 - T_1) = C_{wf}E_L(T_6 - T_L) \quad (2)$$

$$Q_{Kc} = C_{wf}(T_4 - T_5) = C_{wf}E_g(T_4 - T_g') \quad (3)$$

$$Q_{Kh} = C_{wf}(T_5 - T_6) = C_{wf}E_h(T_5 - T_h) \quad (4)$$

where C_{wf} is the constant thermal capacity rate, and $E_i (i = H, g, h, L)$ is the effectiveness of each HE. E_i is defined as:

$$E_i = 1 - e^{-N_i} (i = H, g, h, L) \quad (5)$$

where N_i is the number of heat transfer unit of each HE, and it can be given as:

$$N_i = U_i / C_{wf} \quad (i = H, g, h, L) \tag{6}$$

where U_i is the HC of each HE.

When the Brayton cycle is endoreversible one, the following relationship is satisfied:

$$T_2 / T_1 = T_3 / T_4 = x \tag{7}$$

where $x = \pi^{\frac{k-1}{k}}$ is the isentropic temperature ratio, π is the pressure ratio of process 1-2, and k is the specific heat ratio of the working fluid.

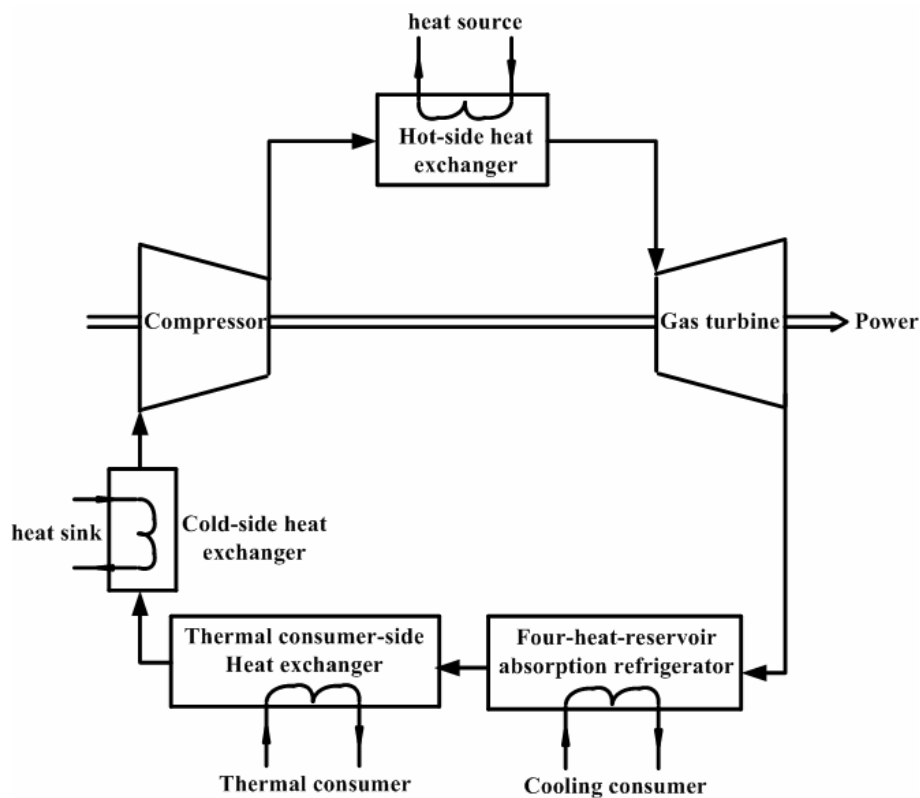


Figure 1. Schematic diagram of CCHPP.

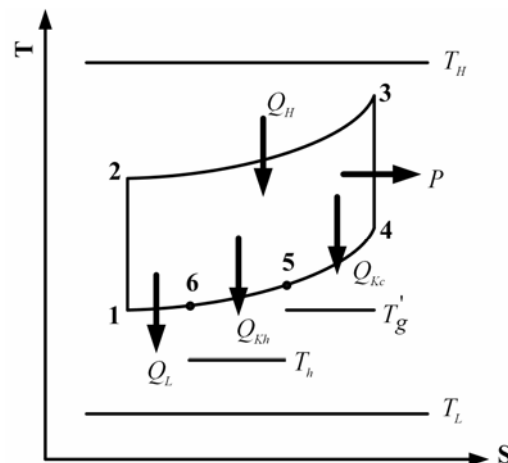


Figure 2. T-s diagram of heating and power generation of CCHPP.

Figure 3 shows an EFHRARC driven by the heat transfer rate Q_{Kc} . There exit four parts in the refrigerator, i.e., generator, absorber, condenser and evaporator, and the temperatures of which are T_g' , T_a' , T_c' and T_e' , respectively. The heat transfer rate between the working fluid of the refrigerator and temperature T_a' is Q_a , and those of the temperatures T_c' and T_e' are Q_c and Q_e , respectively.

The heat transfer equations in the EFHRARC are:

$$Q_a = U_a(T_a' - T_a) \tag{8}$$

$$Q_c = U_c(T_c' - T_c) \tag{9}$$

$$R = Q_e = U_e(T_e - T_e') \tag{10}$$

where R is the cooling load, and U_j ($j = a, c, e$) is the HC of each HE. When the power input of the solution pump is ignored [51-55], the COP and heat distribution released to T_a and T_c are given as:

$$\varepsilon = Q_e / Q_{Kc} \tag{11}$$

$$n = Q_a / Q_c \tag{12}$$

When the EFHRARC is endoreversible one, the following relationships are satisfied:

$$Q_{Kc} + Q_e - Q_a - Q_c = 0 \tag{13}$$

$$Q_{Kc} / T_g' + Q_e / T_e' - Q_a / T_a' - Q_c / T_c' = 0 \tag{14}$$

From Eqs. (3) and (8)-(14), the relationship between R and Q_{Kc} can be expressed as [51]:

$$U_c(Q_{Kc} + R) / [Q_{Kc} + R + U_c T_c (n+1)] + n U_a(Q_{Kc} + R) / [n(Q_{Kc} + R) + U_a T_a (n+1)] = U_e R / (U_e T_e - R) + C_{wf} Q_{Kc} E_g / (C_{wf} E_g T_4 - Q_{Kc}) \tag{15}$$

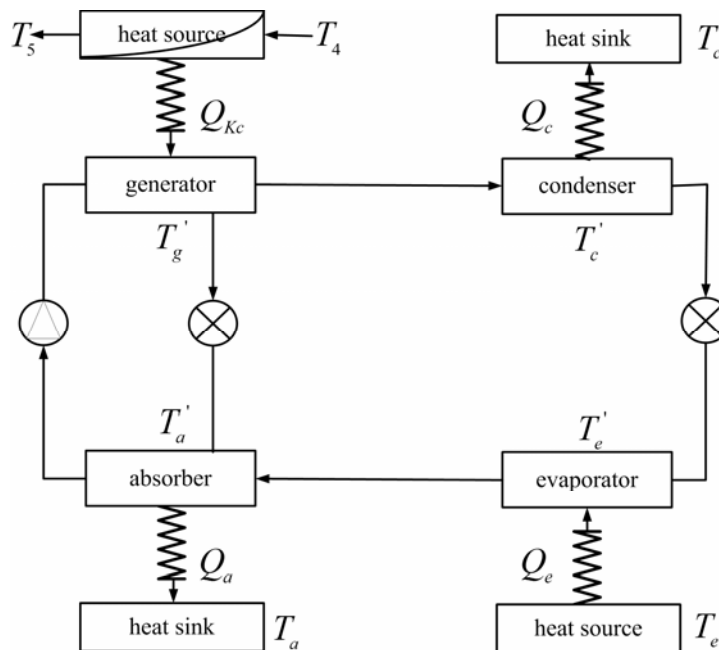


Figure 3. EFHRARC model.

3. Performance analyses

The power output of CCHPP can be obtained based on its energy balance equation:

$$P = Q_H - Q_L - Q_{Kh} - Q_{Kc} \quad (16)$$

The temperatures and heat transfer rates can be obtained by combining Eqs. (1)-(4), (7) and (16):

$$T_1 = \frac{\omega_h T_H E_H (1 - E_h)(1 - E_L)(x - 1)x^{-1} + E_h(T_h - E_L T_h + E_L T_L)}{E_h + \omega_h E_H (1 - E_h)(1 - E_L)(x - 1)} \quad (17)$$

$$T_4 = \frac{\omega_h T_H E_H (1 - E_L)(1 + E_h)(1 - x^{-1}) + E_h(1 - E_H)(T_h - E_L T_h + E_L T_L) + E_h E_H T_H x^{-1}}{E_h + \omega_h E_H (1 - E_h)(1 - E_L)(x - 1)} \quad (18)$$

$$T_5 = \frac{T_h E_h + \omega_h (x - 1) E_H [T_H x^{-1} - T_h E_h (1 - E_L) - T_L E_L]}{E_h + \omega_h E_H (1 - E_h)(1 - E_L)(x - 1)} \quad (19)$$

$$Q_H = \frac{C_{wf} E_H E_h [T_H - x(T_h - E_L T_h + E_L T_L)]}{E_h + \omega_h E_H (1 - E_h)(1 - E_L)(x - 1)} \quad (20)$$

$$Q_L = \frac{C_{wf} E_L [E_h(T_h - T_L) + \omega_h E_H (1 - E_h)(x - 1)(T_H x^{-1} - T_L)]}{E_h + \omega_h E_H (1 - E_h)(1 - E_L)(x - 1)} \quad (21)$$

$$Q_{Kc} = \frac{T_H E_H E_h x^{-1} C_{wf} [1 - \omega_h (1 - E_L)(x - 1)] + T_h E_h E_H C_{wf} (1 - E_L) [\omega_h (x - 1) - 1] + \omega_h E_H E_L C_{wf} (T_L - T_H x^{-1})(x - 1) - E_h E_L C_{wf} (T_h - T_L + T_L E_H)}{E_h + \omega_h E_H (1 - E_h)(1 - E_L)(x - 1)} \quad (22)$$

$$Q_{Kh} = \frac{\omega_h E_H E_h C_{wf} (x - 1) (T_H x^{-1} - T_h + T_h E_L - E_L T_L)}{E_h + \omega_h E_H (1 - E_h)(1 - E_L)(x - 1)} \quad (23)$$

$$P = \frac{E_H E_h C_{wf} (x - 1) (T_H x^{-1} - T_h + T_h E_L - E_L T_L)}{E_h + \omega_h E_H (1 - E_h)(1 - E_L)(x - 1)} \quad (24)$$

where ω_h is the ratio of Q_{Kh} to P [29], which is set as constant in the equations.

The EOR brought by the power is:

$$EX_P = P = \frac{E_H E_h C_{wf} (x - 1) (T_H x^{-1} - T_h + T_h E_L - E_L T_L)}{E_h + \omega_h E_H (1 - E_h)(1 - E_L)(x - 1)} \quad (25)$$

The cooling EOR brought by the EFHRARC is:

$$EX_{Kc} = R(T_0 / T_e - 1) \quad (26)$$

where T_0 is the surrounding temperature, and R can be obtained by substituted Eqs. (5), (6), (18) and (22) into Eq. (15). The analytical solution is hard to apply in the calculation, and numerical solution is adopted instead.

The thermal EOR brought to the thermal consumer is [35]:

$$EX_{Kh} = Q_{Kh}(1 - T_0 / T_h) = \frac{\omega_h E_H E_h C_{wf} (x-1)(T_h - T_0)(T_H x^{-1} - T_h + T_h E_L - E_L T_L)}{T_h E_h + \omega_h T_h E_H (1 - E_h)(1 - E_L)(x-1)} \tag{27}$$

The exergy input and output rates of the whole CCHPP are:

$$EX_I = Q_H(1 - T_0 / T_H) - Q_L(1 - T_0 / T_L) \tag{28}$$

$$EX = EX_P + EX_{Kh} + EX_{Kc} \tag{29}$$

From Eqs. (25)-(27) and (29), the dimensionless EX can be given as:

$$\frac{EX}{C_{wf} T_0} = \frac{E_H E_h (1 + \omega_h - \omega_h \tau_h^{-1})(x-1)(\tau_H x^{-1} - \tau_h + \tau_h E_L - E_L \tau_L) + C_{wf}^{-1} T_0^{-1} R(\tau_c^{-1} - 1)[E_h + \omega_h E_H (1 - E_h)(1 - E_L)(x-1)]}{E_h + \omega_h E_H (1 - E_h)(1 - E_L)(x-1)} \tag{30}$$

where $\tau_H = T_H / T_0$, $\tau_h = T_h / T_0$, $\tau_L = T_L / T_0$ and $\tau_c = T_c / T_0$ are the temperature ratios.

From Eqs. (28) and (29), the EE of the CCHPP can be given as:

$$\eta = EX / EX_I \tag{31}$$

Substituting Eqs. (20), (21), (28) and (29) into (31) yields:

$$\eta = \frac{E_H E_h (1 + \omega_h - \omega_h \tau_h^{-1})(x-1)(\tau_H x^{-1} - \tau_h + \tau_h E_L - E_L \tau_L) + T_0^{-1} C_{wf}^{-1} R(\tau_c^{-1} - 1)[E_h + \omega_h E_H (1 - E_h)(1 - E_L)(x-1)]}{E_H E_L [(1 - \tau_H^{-1})E_h x(\tau_h - \tau_L) + \omega_h (1 - x^{-1} \tau_H \tau_L^{-1})(\tau_L - 1)(1 - E_h)(x-1)] + E_h E_L (1 - \tau_L)(\tau_h \tau_L^{-1} - 1) - E_H E_h (\tau_H^{-1} - 1)(\tau_H - \tau_h x)} \tag{32}$$

The model of the CCHPP includes many special cases. When $\omega_h = 0$ and $Q_{Kc} = 0$, the CCHPP is simplified into single Brayton cycle; when $\omega_h = 0$ and $Q_{Kc} \neq 0$, it is simplified into the cogeneration cycle with cooling and power plants; when $\omega_h \neq 0$ and $Q_{Kc} = 0$, it is simplified into the CHP plant.

4. Performance optimizations

From Eq. (30), when the parameters (τ_H , τ_h , τ_L , τ_c , T_0 , ω_h and n) are specified, the dimensionless exergy output rate (DEOR) of CCHPP is related to the pressure ratio (π) and HCs U_i ($i = H, L, h, g, a, c, e$). When $U_g = U_a = U_c = U_e = U_h = 2kW / K$ and $U_H + U_L = 10kW / K$, the effects of pressure ratio π and HCD $u_H (= U_H / (U_H + U_L))$ on the DEOR are shown in Figure 4. One can see that u_H and π can be optimized, and DEOR has its maximum. Similarly, when the total HC U_T of the HE is fixed, i.e. $U_H + U_L + U_h + U_g + U_a + U_c + U_e = U_T$, U_i ($i = H, L, h, g, a, c, e$) can be also optimized simultaneously. Using the similar method adopted for performance optimizations of gas turbine closed-cycle CHP plants [29-47], the DEOR of the CCHPP will be maximized by taking π and U_i ($i = H, L, h, g, a, c, e$) as optimization variables, respectively.

The HCDs of the HEs are given as:

$$u_H = U_H / U_T, \quad u_L = U_L / U_T, \quad u_h = U_h / U_T, \quad u_g = U_g / U_T, \tag{33}$$

$$u_a = U_a / U_T, \quad u_c = U_c / U_T, \quad u_e = U_e / U_T$$

The following conditions should be satisfied:

$$\begin{aligned} 0 < u_H < 1, \quad 0 < u_L < 1, \quad 0 < u_h < 1, \quad 0 < u_g < 1, \quad 0 < u_a < 1 \\ 0 < u_c < 1, \quad 0 < u_e < 1, \quad u_H + u_L + u_h + u_g + u_a + u_c + u_e = 1 \end{aligned} \quad (34)$$

The HCs can be rewritten as:

$$\begin{aligned} U_H &= u_H U_T, \quad U_L = (1 - u_H - u_h - u_g - u_a - u_c - u_e) U_T, \quad U_h = u_h U_T \\ U_g &= u_g U_T, \quad U_a = u_a U_T, \quad U_c = u_c U_T, \quad U_e = u_e U_T \end{aligned} \quad (35)$$

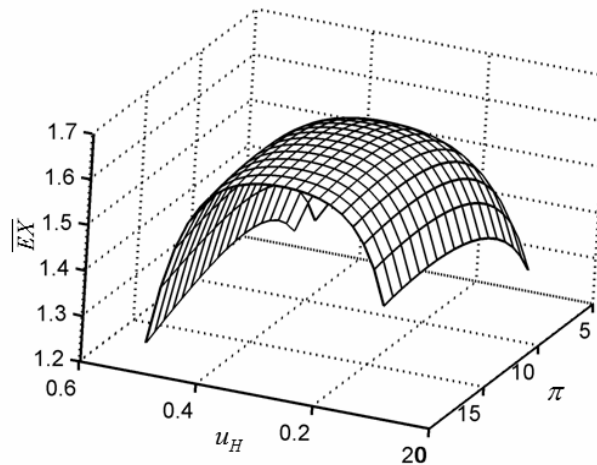


Figure 4. Characteristic of \overline{EX} versus u_H and π .

The temperature constraints of the CCHPP are given as follows:

$$\begin{aligned} T_L < T_1, \quad T_1 < T_2, \quad T_2 < T_3, \quad T_3 < T_H, \quad T_1 < T_6, \quad T_h < T_6 \\ T_6 < T_5, \quad T_5 < T_4, \quad T_4 < T_3, \quad T_1 + T_3 - T_2 - T_4 > 0 \end{aligned} \quad (36)$$

Figure 5 shows the optimization flow chart for DEOR. The optimization steps are given as follows:

- (1) The initial values of the parameters and variables ($u_H, u_h, u_g, u_a, u_c, u_e$ and π) are set.
- (2) The HCs are calculated based on Eq. (35). If Eqs. (34) and (36) are satisfied, the program can continue, else return to the step of initial values.
- (3) The cooling load of the EFHRARC and DEOR are calculated based on Eqs. (15) and (30).
- (4) The maximum DEOR is searched based on Powell arithmetic. If the maximum DEOR is obtained, the program can continue, else return to the step of initial values.
- (5) The optimal results of the CCHPP are obtained. The maximum DEOR, optimal HCDs and pressure ratio are exported.

5. Numerical examples

In the numerical examples, the parameters of the CCHPP are set as: $U_T = 20 \text{ kW/K}$, $k = 1.4$, $C_{wf} = 1.0 \text{ kW/K}$, $\tau_H = 5$, $\tau_h = 1.2$, $\tau_L = 1$, $\omega_h = 0.5$, $n = 1$, $T_e = 280 \text{ K}$, $T_c = 303 \text{ K}$, $T_a = 303 \text{ K}$, and $T_0 = 303 \text{ K}$.

Figure 6 shows the characteristics of the optimal DEOR \overline{EX}_{opt} and optimal HCDs ($(u_H)_{opt}$, $(u_L)_{opt}$, $(u_h)_{opt}$, $(u_g)_{opt}$, $(u_a)_{opt}$, $(u_c)_{opt}$ and $(u_e)_{opt}$) versus pressure ratio π . One can see that \overline{EX}_{opt} has its maximum value (\overline{EX}_{max}), and the corresponding optimal π and HCDs are signed as $\pi_{\overline{EX}}$ and $(u_i)_{\overline{EX}}$ ($i = H, L, h, g, a, c, e$), respectively. Figure 7 shows the effect of the ratio ω_h on the optimal DEOR (\overline{EX}_{opt}) versus EE $\eta_{\overline{EX}_{opt}}$ characteristic. It indicates that \overline{EX}_{opt} has its maximum value (\overline{EX}_{max}), and \overline{EX}_{max} increases when the ratio ω_h increases.

The characteristics of the HCDs $(u_i)_{\overline{EX}}$ ($i = H, L, h, g, a, c, e$) and $\pi_{\overline{EX}}$ versus τ_H and U_T are shown in Figures 8 and 9, respectively. The effects of τ_h , τ_c and ω_h on the optimal variables are also numerically analyzed. They indicate that $(u_H)_{\overline{EX}}$ and $(u_L)_{\overline{EX}}$ are larger than $(u_h)_{opt}$, $(u_g)_{opt}$, $(u_a)_{opt}$, $(u_c)_{opt}$ and $(u_e)_{opt}$; due to the heat distribution $n = 1$, the curves of $(u_a)_{\overline{EX}}$ and $(u_c)_{\overline{EX}}$ coincide with each other; when τ_H increases, $(u_g)_{\overline{EX}}$, $(u_a)_{\overline{EX}}$, $(u_c)_{\overline{EX}}$ and $(u_e)_{\overline{EX}}$ decrease, and $(u_H)_{\overline{EX}}$, $(u_h)_{\overline{EX}}$, $(u_L)_{\overline{EX}}$ and $(\pi)_{\overline{EX}}$ increase; when τ_h increases, $(u_g)_{\overline{EX}}$, $(u_a)_{\overline{EX}}$, $(u_c)_{\overline{EX}}$, $(u_e)_{\overline{EX}}$ and $(\pi)_{\overline{EX}}$ decrease, and $(u_H)_{\overline{EX}}$, $(u_h)_{\overline{EX}}$ and $(u_L)_{\overline{EX}}$ increase; when τ_c increases, $(u_g)_{\overline{EX}}$, $(u_a)_{\overline{EX}}$, $(u_c)_{\overline{EX}}$, $(u_e)_{\overline{EX}}$ and $(u_h)_{\overline{EX}}$ decrease, and $(u_H)_{\overline{EX}}$, $(u_L)_{\overline{EX}}$ and $(\pi)_{\overline{EX}}$ increase; when ω_h increases, $(u_g)_{\overline{EX}}$, $(u_a)_{\overline{EX}}$, $(u_c)_{\overline{EX}}$, $(u_e)_{\overline{EX}}$, $(u_L)_{\overline{EX}}$ and $(\pi)_{\overline{EX}}$ decrease, and $(u_H)_{\overline{EX}}$ as well as $(u_h)_{\overline{EX}}$ increase; when U_T increases, $(u_g)_{\overline{EX}}$, $(u_a)_{\overline{EX}}$, $(u_c)_{\overline{EX}}$ and $(u_e)_{\overline{EX}}$ increase, and $(u_H)_{\overline{EX}}$, $(u_L)_{\overline{EX}}$ and $(\pi)_{\overline{EX}}$ decrease. Meanwhile, U_T has no obvious effect on $(u_h)_{\overline{EX}}$.

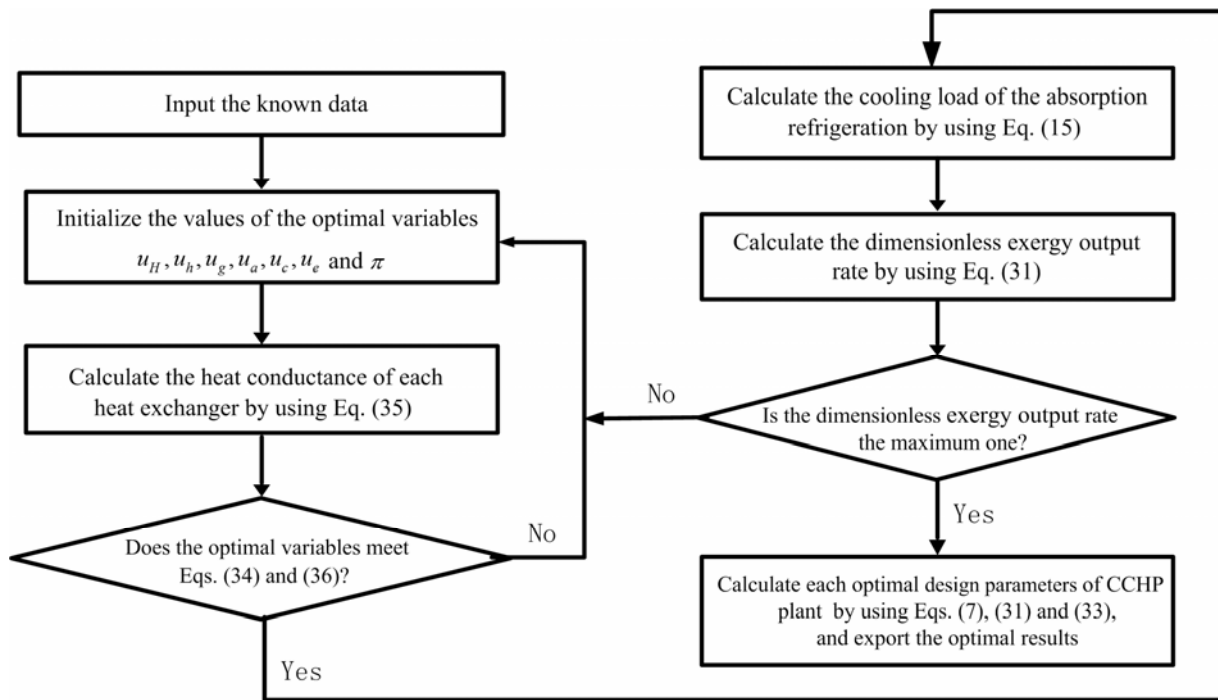


Figure 5. Flow chart of exergy output rate optimization routine.

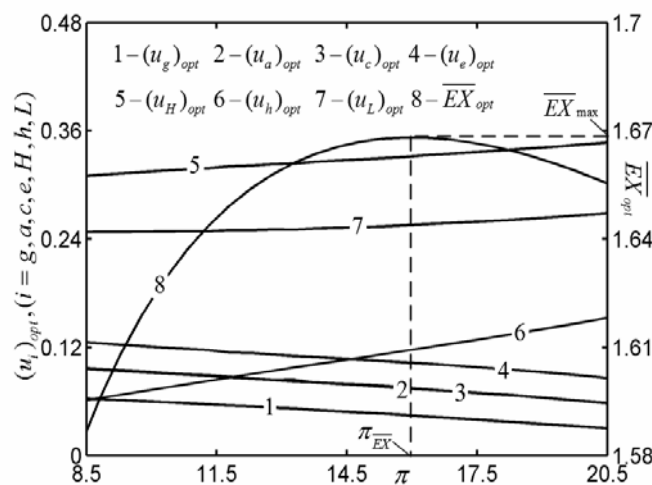


Figure 6. Characteristics of $(u_g)_{opt}$, $(u_a)_{opt}$, $(u_c)_{opt}$, $(u_e)_{opt}$, $(u_H)_{opt}$, $(u_h)_{opt}$, $(u_L)_{opt}$ and \overline{EX}_{opt} versus π .

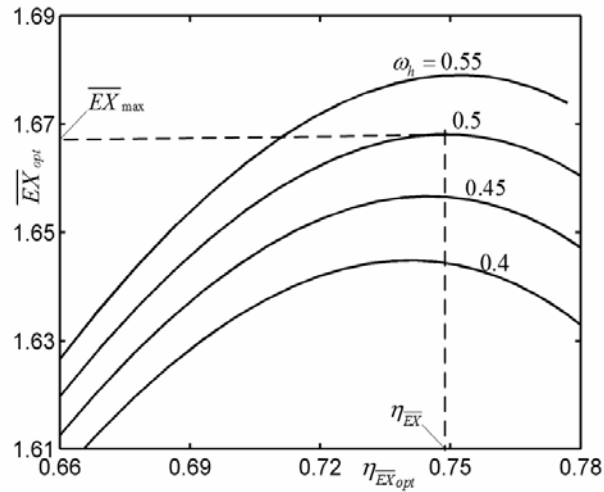


Figure 7. Effect of ω_h on $\bar{\Pi}_{opt}$ versus $\eta_{\bar{\Pi}_{opt}}$ characteristic.

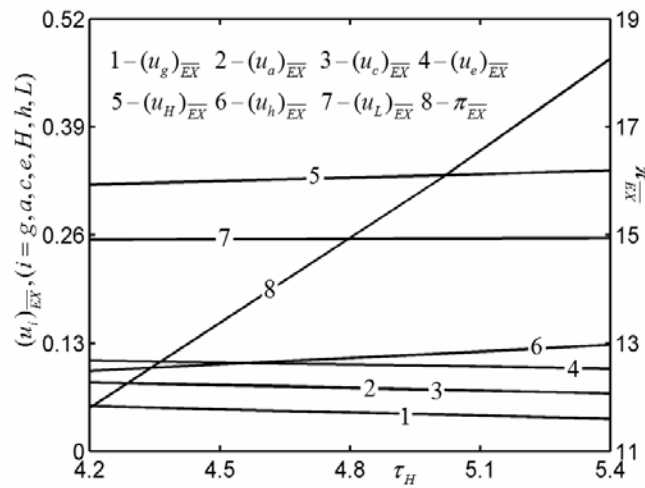


Figure 8. Characteristics of $(u_g)_{EX}$, $(u_a)_{EX}$, $(u_c)_{EX}$, $(u_e)_{EX}$, $(u_H)_{EX}$, $(u_h)_{EX}$, $(u_L)_{EX}$ and π_{EX} versus τ_H .

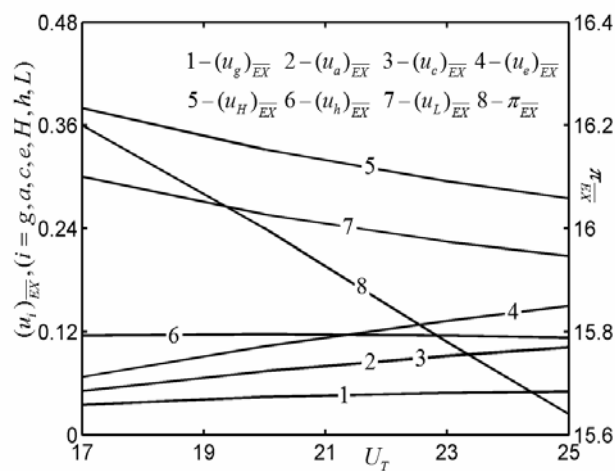


Figure 9. Characteristics of $(u_g)_{EX}$, $(u_a)_{EX}$, $(u_c)_{EX}$, $(u_e)_{EX}$, $(u_H)_{EX}$, $(u_h)_{EX}$, $(u_L)_{EX}$ and π_{EX} versus U_T .

The characteristics of \overline{EX}_{\max} and $\eta_{\overline{EX}}$ versus τ_H and U_T are shown in Figures 10 and 11, respectively. The effects of τ_h , τ_c and ω_h on \overline{EX}_{\max} and $\eta_{\overline{EX}}$ are also numerically analyzed. They indicate that with the increases in τ_H , τ_h and ω_h , both \overline{EX}_{\max} and $\eta_{\overline{EX}}$ increase; with the increases in τ_c , \overline{EX}_{\max} decreases, and $\eta_{\overline{EX}}$ increases; with the increases in U_T , \overline{EX}_{\max} increases, and $\eta_{\overline{EX}}$ increases a little at first, then decreases a little, that is, U_T only has a slight effect on $\eta_{\overline{EX}}$.

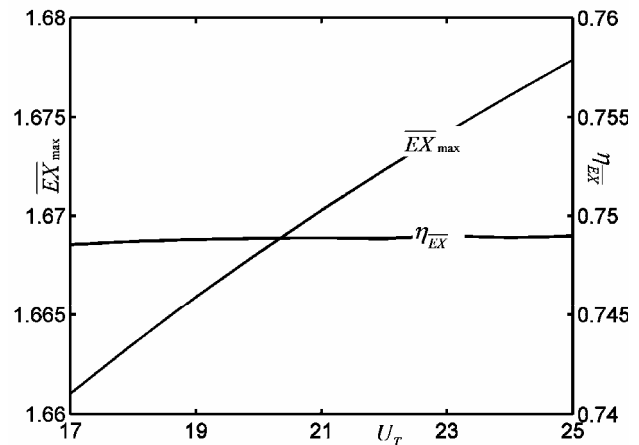
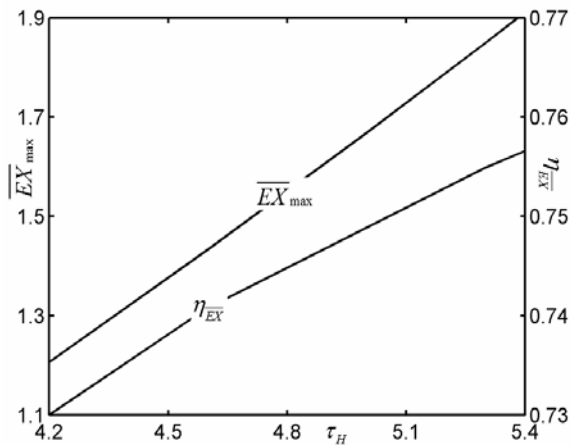


Figure 10. Characteristics of \overline{EX}_{\max} and $\eta_{\overline{EX}}$ versus τ_H . Figure 11. Characteristics of \overline{EX}_{\max} and $\eta_{\overline{EX}}$ versus U_T .

6. Conclusions

Based on FTT, a CCHPP, composed of an ECBC and EFHRARC, is studied in this paper. The DEOR and EE performances are optimized. It indicates that DEOR has its maximum value (\overline{EX}_{\max}), and the optimization variables π and HCDs reach their optimal values, respectively. The HCDs $(u_H)_{\overline{EX}}$ and $(u_L)_{\overline{EX}}$ are larger than $(u_h)_{opt}$, $(u_g)_{opt}$, $(u_a)_{opt}$, $(u_c)_{opt}$ and $(u_e)_{opt}$. Due to the heat distribution $n=1$, the curves of $(u_a)_{\overline{EX}}$ and $(u_c)_{\overline{EX}}$ coincide with each other. The effects of τ_H , τ_h , τ_c , ω_h and U_T on the optimal performances of the CCHPP are also analyzed. This paper uses FTT to investigate the optimal exergy performance of a CCHPP theoretically, which enriches FTT theory. Moreover, many ideal assumptions are made in the model of this paper, one can further build more practical model to carry out optimization of the CCHPP.

Acknowledgment

This work is supported by the National Natural Science Foundation of China (Grant No. 51576207).

Nomenclature

- C heat capacity rate (kW / K)
- E heat exchanger effectiveness
- EX exergy output rate (EOR) (kW)
- \overline{EX} dimensionless EOR
- EX_p EOR brought by the power (kW)
- EX_{Kc} cooling EOR brought by EFHRARC (kW)
- EX_h thermal EOR brought to the thermal consumer (kW)
- EX_I total EOR of the CCHPP (kW)
- N heat transfer unit number
- n total heat distribution
- P power output of CCHPP (kW)

Q	heat transfer rate (kW)
T	temperature (K)
U	heat conductance (kW / K)
u	heat conductance distribution
x	isentropic temperature ratio

Greek symbols

ε	performance coefficient of the EFHRARC
η	exergy efficiency
π	pressure ratio
ω_h	heat ratio
τ	temperature ratio

Subscripts

a	absorber-side
c	condenser-side
e	evaporator-side/cooling consumer-side
g	generator-side
H	hot-side
h	thermal consumer-side
I	total exergy input rate
L	cold-side
max	maximum
opt	optimal
T	total
wf	working fluid
\overline{EX}	maximum dimensionless EOR
\overline{EX}_{opt}	optimal dimensionless EOR
0	ambient
1,2,3,4,5,6	state points of the cycle

References

- [1] Rezaie, B. and Rosen, M.A., "District heating and cooling: Review of technology and potential enhancements," *Appl. Energy*, 93(93), pp. 2-10, (2012).
- [2] Cho, H., Smith, A.D. and Mago, P., "Combined cooling, heating and power: A review of performance improvement and optimization," *Appl. Energy*, 136, pp. 168-185, (2014).
- [3] Lozano, M.A., Carvalho, M., Ramos, J.C. and Serra, L.M., "Thermoeconomic analysis of simple trigeneration systems," *Int. J. Thermodyn.*, 12(3), pp. 147-153, (2009).
- [4] Zheng, C.Y., Wu, J.Y. and Zhai, X.Q., "A novel operation strategy for CCHP systems based on minimum distance," *Appl. Energy*, 128(128), pp. 325-335, (2014).
- [5] Wang, J.J., Yang, K. and Xu, Z.L., "Chao F. Energy and exergy analyses of an integrated CCHP system with biomass air gasification," *Appl. Energy*, 142, pp. 317-327, (2015).
- [6] Ju, L., Tan, Z., Li, H., Tan, Q., Yu, X. and Song, X., "Multi-objective operation optimization and evaluation model for CCHP and renewable energy based hybrid energy system driven by distributed energy resources in china," *Energy*, 111, pp. 322-340, (2016).
- [7] Andresen, B., *Finite Time Thermodynamics*, University of Copenhagen: Physics Laboratory II, (1983).
- [8] Bejan, A., "Entropy generation minimization: The new thermodynamics of finite-size device and finite-time processes," *J. Appl. Phys.*, 79(3), pp. 1191-1218, (1996).
- [9] Berry, R.S. and Kazakov, V.A., Sieniutycz, S., Szwast, Z. and Tsirlin, A.M., *Thermodynamic Optimization of Finite Time Processes*, Chichester: Wiley, (1999).
- [10] Chen, L.G., Wu, C. and Sun, F.R., "Finite time thermodynamic optimization or entropy generation minimization of energy systems," *J. Non-Equilib. Thermodyn.*, 24(4), pp. 327-359, (1999).
- [11] Wu, C., Chen, L.G. and Chen, J.C., *Recent Advances in Finite Time Thermodynamics*, New York: Nova Science Publishers, (1999).

- [12] Chen, L.G. and Sun, F.R., *Advances in Finite Time Thermodynamics: Analysis and optimization*, New York: Nova Science Publishers, (2004).
- [13] Chen, L.G., *Finite-Time Thermodynamic Analysis of Irreversible Processes and Cycles*, Beijing: High Education Press, (2005).
- [14] Andresen, B., "Current trends in finite-time thermodynamics," *Angewandte Chemie International Edition*, 50(12), pp. 2690-2704, (2011).
- [15] Feidt, M., "Thermodynamics of energy systems and processes: A review and perspectives," *J. Appl. Fluid Mech.*, 5(2), pp. 85-98, (2012).
- [16] Feidt, M., "Evolution of thermodynamic modelling for three and four heat reservoirs reverse cycle machines: A review and new trends," *Int. J. Refrigeration*, 36(1), pp. 8-23, (2013).
- [17] Qin, X.Y., Chen, L.G., Ge, Y.L. and Sun, F.R., "Finite time thermodynamic studies on absorption thermodynamic cycles: A state of the arts review," *Arabian J. S. Eng.*, 38(3), pp. 405-419, (2013).
- [18] Le, Roux.W.G., Bello-Ochende, T. and Meyer, J.P., "A review on the thermodynamic optimisation and modelling of the solar thermal Brayton cycle," *Renew. Sustain. Energy Rev.*, 28, pp. 677-690, (2013).
- [19] Sieniutycz, S. and Jezowski, J., *Energy Optimization in Process Systems and Fuel Cells*, Oxford: Elsevier, (2013).
- [20] Ngouateu, Wouagfack, P.A. and Tchinda, R., "Finite-time thermodynamics optimization of absorption refrigeration systems: A review," *Renew. Sustain. Energy Rev.*, 21, pp. 524-536, (2013).
- [21] Li, J., Chen, L.G., Ge, Y.L. and Sun, F.R., "Progress in the study on finite time thermodynamic optimization for direct and reverse two-heat-reservoir thermodynamic cycles," *Acta Physica Sinica*, 62(13), pp. 130501, (2013).
- [22] Ding, Z.M., Chen, L.G., Wang, W.H. and Sun, F.R., "Progress in study on finite time thermodynamic performance optimization for three kinds of microscopic energy conversion systems," *Sci. China: Tech. Sci.*, 45(9), pp. 889-918, (2015).
- [23] Hoffmann, K.H., Andresen, B. and Salamon, P., "Finite-time thermodynamics tools to analyze dissipative processes," *Proceedings of The 240 Conference: Science's Great Challenges, Advances in Chemical Physics*, 157, pp. 57-67, (2015).
- [24] Chen, L.G., Meng, F.K. and Sun, F.R., "Thermodynamic analyses and optimizations for thermoelectric devices: The state of the arts," *Sci. China: Tech. Sci.*, 59(3), pp. 442-455, (2016).
- [25] Ge, Y.L., Chen, L.G. and Sun, F.R., "Progress in finite time thermodynamic studies for internal combustion engine cycles," *Entropy*, 18(4), pp. 139, (2016).
- [26] Chen, L.G. and Xia, S.J., *Generalized Thermodynamic Dynamic-Optimization for Irreversible Processes*, Beijing: Science Press, (2016) (in Chinese).
- [27] Chen, L.G. and Xia, S.J., *Generalized Thermodynamic Dynamic-Optimization for Irreversible Cycles*, Beijing: Science Press, 2016 (in Chinese).
- [28] Chen, L.G., Feng, H.J. and Xie, Z.H., "Generalized Thermodynamic Optimization for Iron and Steel Production Processes: Theoretical Exploration and Application Cases," *Entropy*, 18(10), pp. 353, (2016).
- [29] Yilmaz, T., "Performance optimization of a gas turbine-based cogeneration system," *J. Phys. D: Appl. Phys.*, 39(11), pp. 2454-2458, (2006).
- [30] Hao, X.L. and Zhang, G.Q., "Maximum useful energy-rate analysis of an endoreversible Joule-Brayton cogeneration cycle," *Appl. Energy*, 84(11), pp. 1092-1101, (2007).
- [31] Hao, X. and Zhang, G., "Exergy Optimization of a Brayton cycle-based cogeneration plant," *Int. J. Exergy*, 6(1), 34-38, (2009).
- [32] Ust, Y., Sahin, B. and Yilmaz, T., "Optimization of a regenerative gas-turbine cogeneration system based on a new exergetic performance criterion: Exergetic performance coefficient," *Proc. IMechE, Part A: J. Power Energy*, 221(4), 447-458, (2007).
- [33] Ust, Y., Sahin, B. and Kodali, A., "Optimization of a dual cycle cogeneration system based on a new exergetic performance criterion," *Appl. Energy*, 84(11), pp. 1079-1091, (2007).
- [34] Ust, Y., Arslan, F., Ozsari, I. and Cakir, M., "Thermodynamic performance analysis and optimization of DMC (Dual Miller Cycle) cogeneration system by considering exergetic performance coefficient and total exergy output criteria," *Energy*, 90, pp. 552-559, (2015).
- [35] Tao, G., Chen, L.G., Sun, F.R. and Wu, C., "Exergoeconomic performance optimization for an endoreversible simple gas turbine closed-cycle cogeneration plant," *Int. J. Ambient Energy*, 30(3), pp. 115-124, (2009).

- [36] Tao, G., Chen, L.G. and Sun, F.R., "Exergoeconomic performance optimization for an endoreversible regenerative gas turbine closed-cycle cogeneration plant," *Rev. Mex. Fis.*, 55(3), pp. 192-200, (2009).
- [37] Chen, L.G., Tao, G. and Sun, F.R., "Finite time exergoeconomic optimal performance for an irreversible gas turbine closed-cycle cogeneration plant," *Int. J. Sustain. Energy*, 31(1), pp. 43-58, (2012).
- [38] Chen, L.G., Yang, B., Sun, F.R. and Wu, C., "Exergetic performance optimization of an endoreversible intercooled regenerated Brayton cogeneration plant. Part 1: thermodynamic model and parametric analysis," *Int. J. Ambient Energy*, 32(3), pp. 116-123, (2011).
- [39] Yang, B., Chen, L.G. and Sun, F.R., "Exergoeconomic performance analyses of an endoreversible intercooled regenerative Brayton cogeneration type model," *Int. J. Sustain. Energy*, 30(2), pp. 65-81, (2011).
- [40] Yang, B., Chen, L.G., Sun, F.R. and Wu, C., "Exergetic performance optimization of an endoreversible intercooled regenerated Brayton cogeneration plant. Part 2: exergy output rate and EE optimization," *Int. J. Ambient Energy*, 33(2), pp. 98-104, (2012).
- [41] Yang, B., Chen, L.G. and Sun, F.R., "Exergoeconomic performance optimization of an endoreversible intercooled regenerative Brayton combined heat and power plant coupled to variable-temperature heat reservoirs," *Int. J. Energy Environ.*, 3(4), pp. 505-520, (2012).
- [42] Yang, B., Chen, L.G. and Sun, F.R., "Exergy performance optimization of an endoreversible variable-temperature heat reservoirs intercooled regenerated Brayton cogeneration plant," *J. Energy Inst.*, 89(1), pp. 1-11, (2016).
- [43] Yang, B., Chen, L.G. and Sun, F.R., "Finite time exergoeconomic performance of an irreversible intercooled regenerative Brayton cogeneration plant," *J. Energy Inst.*, 84(1), pp. 5-12, (2011).
- [44] Yang, B., Chen, L.G., Ge, Y. and Sun F.R. "Exergy performance optimization of an irreversible closed intercooled regenerative Brayton cogeneration plant," *Arabian J. Sci. Eng.*, 39(8), pp. 6385-6397, (2014).
- [45] Yang, B., Chen, L.G., Ge, Y.L. and Sun F.R., "Exergy performance analyses of an irreversible two-stage intercooled regenerative reheated closed Brayton CHP plant," *Int. J. Exergy*, 14(4), pp. 459-483, (2014).
- [46] Chen, L.G., Yang, B., Ge, Y.L. and Sun F.R., "Finite time exergoeconomic performance of a real, intercooled, regenerated gas turbine cogeneration plant. Part 1: model description and parametric analyses," *Int. J. Low-Carbon Tech.*, 9(1), pp. 29-37, (2014).
- [47] Yang, B., Chen, L.G., Ge, Y.L. and Sun F.R., "Finite time exergoeconomic performance of a real intercooled regenerated gas turbine cogeneration plant. Part 2: heat conductance distribution and pressure ratio optimization," *Int. J. Low-Carbon Tech.*, 9(4), pp. 262-267, (2014).
- [48] Yan, Z. and Chen, S., "Finite time thermodynamic performance bounds of a three-heat-reservoir refrigerator," *Chin. Sci. Bull.*, 31(10), pp. 798, (1986).
- [49] Chen, J., "Performance of absorption refrigeration cycle at maximum cooling rate," *Cryogenics*, 34(12), pp. 997-1000, (1994).
- [50] Chen, L.G., Sun, F.R., Chen, W., Tang, K. and Wu, C., "Optimal performance coefficient and cooling load relationship of three-heat-source endoreversible refrigerator," *Int. J. Power & Energy Systems*, 17(3), pp. 206-208, (1997).
- [51] Chen, J., "The optimum performance characteristics of a four-temperature-level irreversible absorption refrigerator at maximum specific cooling load," *J. Phys. D: Appl. Phys.*, 32(24), pp. 3085-3091, (1999).
- [52] Chen, L.G., Zheng, T., Sun, F.R. and Wu, C., "Optimal cooling load and COP relationship of a four-heat-reservoir endoreversible absorption refrigerator cycle," *Entropy*, 6(3), pp. 316-326, (2004).
- [53] Zheng, T., Chen, L.G., Sun, F.R. and Wu, C., "Performance optimization of an irreversible four-heat-reservoir absorption refrigerator," *Appl. Energy*, 76(4), pp. 391-414, (2003).
- [54] Qin, X., Chen, L.G. and Sun, F.R., "Thermodynamic modeling and performance of variable-temperature heat reservoir absorption refrigeration cycle," *Int. J. Exergy*, 7(4), pp. 521-534, (2010).
- [55] Tao, G., Chen, L.G., Sun, F.R. and Wu, C., "Optimization between cooling load and entropy generation rate of an endoreversible four-heat-reservoir absorption refrigerator," *Int. J. Ambient Energy*, 30(1), pp. 27-32, (2009).

- [56] Chen, L.G., Yang, B., Shen, X., Xie, Z.H. and Sun, F.R., "Thermodynamic optimization opportunities for the recovery and utilization of residual energy and heat in China steel industry: A case study," *Appl. Thermal Eng.*, 86, pp. 151-160, (2015).
- [57] Chen, L.G., Feng, H. and Sun, F.R., "Exergoeconomic performance optimization for a combined cooling, heating and power generation plant with an endoreversible closed Brayton cycle," *Math. Comp. Model.*, 54(11-12), pp. 2785-2801, (2011).
- [58] Yang, B., Chen, L.G., Ge, Y.L. and Sun, F.R., "Exergy analyses of an endoreversible closed regenerative Brayton cycle CCHP plant," *Int. J. Energy Environ.*, 5(6), pp. 655-668, (2014).



Huijun Feng received all his degrees (BS, 2008; MS, 2010; PhD, 2014) in power engineering and engineering thermophysics from the Naval University of Engineering, P R China. His work covers topics in engineering thermodynamics and constructal theory. Dr Feng is the author or coauthor of over 90 peer-refereed articles (over 60 in English journals) and 1 book.



Lingen Chen received all his degrees (BS, 1983; MS, 1986; PhD, 1998) in power engineering and engineering thermophysics from the Naval University of Engineering, P R China. His work covers a diversity of topics in engineering thermodynamics, constructal theory, turbomachinery, reliability engineering, and technology support for propulsion plants. He had been the Director of the Department of Nuclear Energy Science and Engineering, the Superintendent of the Postgraduate School, and the Dean of the College of Naval Architecture and Power. Now, he is the Direct, Institute of Thermal Science and Power Engineering, the Director, Military Key Laboratory for Naval Ship Power Engineering, the Direct of the National Experimental Teaching Demonstration Center for Naval Ship Power Engineering, and the Dean of the College of Power Engineering, Naval University of Engineering, P R China. Professor Chen is the author or co-author of over 1630 peer-refereed articles (over 685 in English journals and 75 in international conferences) and 12 books (two in English).
E-mail address: lgchenna@yahoo.com; lingenchen@hotmail.com, Fax: 0086-27-83638709, Tel: 0086-27-83615046



Zhihui Xie received his BS degree (2000) in thermal engineering and MS degree (2005) in environm engineering from Huazhong University of Science and Technology, P R China, and received his PhD de (2010) in power engineering and engineering thermophysics from Naval University of Engineering, China. His work covers topics in engineering thermodynamics, heat transfer and constructal the Professor Xie is the author or co-author of over 60 peer-refereed articles (over 40 in English journals).



Yanlin Ge received all his degrees (BS, 2002; MS, 2005; PhD, 2011) in power engineering and engines thermophysics from the Naval University of Engineering, P R China. His work covers topics in finite thermodynamics and technology support for propulsion plants. Associate Professor Ge is the authc coauthor of over 160 peer-refereed articles (over 70 in English journals).